JOC The Journal of Organic Chemistry

Featured Article

pubs.acs.org/joc

Bis-thioether-Substituted Perylene Diimides: Structural, Electrochemical, and Spectroelectrochemical Properties

Anna G. Slater, E. Stephen Davies, Stephen P. Argent, William Lewis, Alexander J. Blake, Jonathan McMaster, and Neil R. Champness*

School of Chemistry, University of Nottingham, University Park, Nottingham NG7 2RD, U.K.

Supporting Information

ABSTRACT: The synthesis and separation of the 1,6- and 1,7- isomers of *N*,*N*′-bis(alkyl)diadamantylthio-3,4,9,10-perylenetetracarboxylic acid diimide are reported. Investigations of the structural, electrochemical, spectroscopic, and spectroelectrochemical properties of the isomers reveal a sequence of electrochemically and chemically reversible reduction processes for both isomers. Three X-ray crystal structures are reported including a pair of 1,6- and 1,7-isomers demonstrating the twist of the perylene core in the solid state. Our studies thoroughly characterize the mono- and direduced states of the two isomers allowing unequivocal characterization of the reduced species by UV−vis and IR spectroscopic measurements. EPR studies also allow direct identification of the monoreduced PTCDI species and spectroscopic measurements confirm the delocalization of electronic density around the carbonyl moieties of the reduced species.

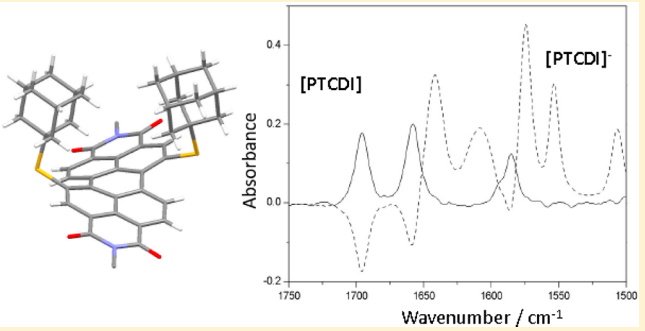

INTRODUCTION

Perylene tetracarboxylic diimides (PTCDIs) and their derivatives have been widely investigated for a variety of applications, due to their remarkable optical and electronic properties.[1] In addition, the wide scope for functionalization of the aromatic core gives great potential for fine-tuning the properties of such compounds. As a result of these attractive qualities, PTCDIs have been synthesized for use in applications as diverse as semiconductors,[2] solar cells,[3] photoactive dye architectures,[4] DNA assays,[5] and liquid crystalline materials.[6] The ability to preserve hydrogen-bonding capability in the perylenes synthesized, when combined with their extended aromatic structure, makes them good candidates for surface absorption and subsequent organization into supramolecular architectures.[7] As many of the applications of PTCDI derivatives exploit their electronic or optical properties it is of particular importance to have a thorough understanding and full characterization of the nature of their various redox states. Our studies have focused on the characterization and exploitation of the reversible interconversion of PTCDI redox states, notably for disubstituted PTCDI species for which isomerism is a notable issue.[7f,8]

Derivatization of the parent perylene dianhydride to a substituted perylenetetracarboxylic diimide can be achieved by two main approaches. First, the imide functionality can be formed using a variety of substituted amines.[7f,9,10] The nature of imide functionalization can be selected to facilitate ongoing synthetic pathways and impart varying degrees of solubility to the typically low solubility of the parent PTCDI compound. Second, imide functionalities of particular interest to those wishing to prepare free imide species[7] are alkoxybenzylamines, including dibutoxybenzylamine (DBOB),[11] which can be cleanly removed to yield free imide in a single step.[7f]

Elucidation of the orbital structure present in PTCDIs reveals a node in both the HOMO and LUMO at the imide position, thus changing the nature of the imide substituent typically has little effect on the electronic properties of the PTCDI; variations in the acceptor and donor orbitals arise mainly from the configuration of the aromatic core.[12] Derivatization of the parent perylene compound in the 1, 6, 7 and/or 12 positions, commonly referred to as the "bay region", can, however, alter the properties of the perylene core significantly, and is a focus of study for those wishing to interrogate the electronic and optical properties of such species.[8,13] The synthesis of bay-substituted species is usually achieved by first introducing halogen substituents[14] and subsequent reaction with a wide range of chemical functionalities.[7f,8,15] This powerful strategy can be exploited to yield mono-, di-, tri-, and tetrasubstituted PTCDIs through choice of halogen and reaction conditions.[14]

Disubstituted PTCDIs are generally synthesized from the corresponding dibrominated perylene species. Such compounds exhibit isomerism; both 1,6- and 1,7-dibromo-PCTDA are produced in the bromination of PTCDA, 3,4,9,10-perylenetetracarboxylic acid dianhydride, in a ratio of 1:4, along with mono-, tri-, and tetrabrominated PTCDA.[10] Substitution at the anhydride moieties with amines improves

Received: January 9, 2013
Published: March 18, 2013

   dx.doi.org/10.1021/jo400026r | J. Org. Chem. 2013, 78, 2853−2862

Scheme 1. Synthesis of Adamantylthio-Substituted PTCDI Derivatives[a]

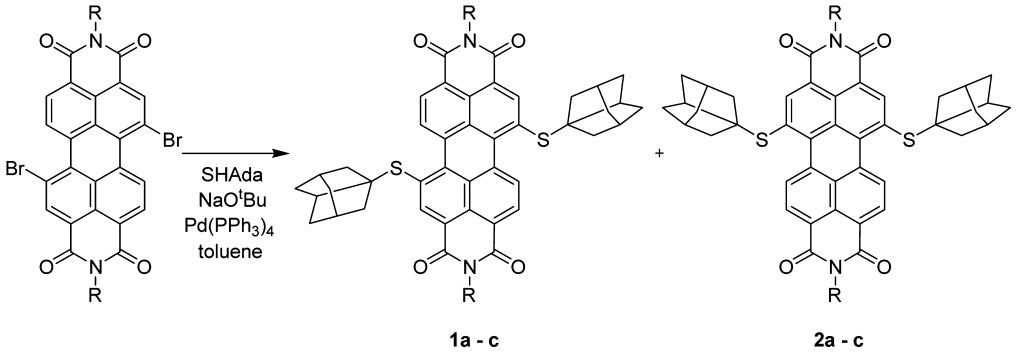

[a]Key: AdaSH, ^{t}BuONa, Pd(PPh$_3$)$_4$, toluene, 80−90 °C, 24 h, under N$_2$. **1a**/**2a**, R = butyl; **1b**/**2b**, R = ethylhexyl; **1c**/**2c**, R = 2,4-dibutoxybenzyl.

solubility and allows purification of the dibrominated species. 1,6- and 1,7-dibromo-PTCDI derivatives are not generally separable unless the imide used facilitates isolation of the 1,7-isomer via repeated recrystallization.[10] However, by limiting the synthetic strategies to a particular imide functionality, subsequent solubility, reactivity, and supramolecular assembly of target materials can be restricted. Unless the 1,6- and 1,7-dibromo-PCTDI isomers are separated, further functionalization of the mixture via nucleophilic substitution yields a mixture of isomers, but in select cases the isomers can be separated.[8a,b]

It has been noted that the electrochemical properties of 1,6- and 1,7-isomers differ significantly where the bay region is substituted with amino groups,[8b,15] and, to a lesser extent, in ferrocenyl systems.[8a] A family of PTCDIs that has been less well studied is the dithio-substituted systems, and although isomerically pure compounds have been isolated,[16] the differences in the properties of the two isomers have rarely been studied in detail. In order to study these differences we have synthesized six compounds comprising three pairs of 1,7- (**1**) and 1,6-isomers (**2**) of diadamantylthio-substituted PTCDI derivatives, each pair possessing a different moiety at the imide position; **1a**/**2a**, R = butyl; **1b**/**2b**, R = ethylhexyl; **1c**/**2c**, R = 2,4-dibutoxybenzyl (Scheme 1). The synthesis of these compounds has allowed a comprehensive examination of the electronic and optical properties of each isomer. A comparison is also drawn with the previously synthesized and studied dithiopropyl-substituted PTCDI, whose isomers were not separated.[7f] Compounds **1a**−**c** and **2a**−**c** represent the first isolated pairs of isomers of dithio-disubstituted PTCDI, and as such we have studied their properties in detail. By using a combination of techniques, particularly UV−visible and IR spectroelectrochemical methods, we have been able to probe the nature of the compound's reduced states giving a full appreciation of the spectroscopic signatures of this important class of molecule.

RESULTS AND DISCUSSION

Six related adamantylthio-substituted PTCDI derivatives were synthesized, comprising three pairs of 1,7- and 1,6-isomers; **1a**−**c** and **2a**−**c** (Scheme 1). Reactions analogous to those used to prepare di(propylthio)-derivatized PTCDI, **3**,[7f] replacing 1-propanethiol with 1-adamantanethiol in the reaction, yielded only a small amount of monosubstituted product along with a large proportion of impurities. Higher temperatures and a variety of alternative solvents and bases were tested with only modest improvements. A modified palladium coupling from a synthesis by Migita and co-workers[17] was therefore used (Scheme 1), as previously reported for **1b**,[18] replacing DMF with toluene and decreasing the reaction times, which was found to give the desired products, **1a**−**c** and **2a**−**c**, in excellent yield in all cases. Significantly, the 1,6- and 1,7-isomers of the product could be separated by column chromatography. Compounds **1a**−**c** and **2a**−**c** were extensively characterized by ^{1}H, ^{13}C, COSY, and HMQC NMR, as well as MALDI-TOF MS and CHN. For comparison to **1** and **2**, *N*,*N*′-bis(*n*-butyl)dipropanethio-3,4:9,10-perylenetetracarboxylic acid diimide, **3**, was prepared according to our previously published route,[7f] yielding an inseparable mix of 1,6- and 1,7-isomers of the product in a ratio of 1:4.

Single crystals were successfully grown of three of the compounds, **1a**, **1c** and **2c**, from a diethyl ether solution of **1a** and through the layering of MeOH over $CHCl_3$ solutions of **1c** and **2c**. The crystals of **1c** and **2c** are one of only two examples of a structurally characterized pair of 1,6- and 1,7-isomers of a disubstituted perylene diimide, the first being one reported by our group in 2009.[8a] As anticipated for 1,7- and 1,6-disubstituted PTCDI derivatives, all three molecules adopted a twisted arrangement of the perylene core, induced by steric interactions between the adamantylthio units and the proton located on the adjacent position of the perylene core; see Figure 1 for the example of **1a**. Interestingly, Würthner et al. have reported[19] an example of a disubstituted PTCDI molecule in which the steric bulk of the 2,6-diphenylphenoxy substituents gives rise to a non-twisted, planar, perylene core in contrast to all previous examples of disubstituted PTCDI derivatives. In the case of the 1,7-derivatives **1a** (Figure 1a) and **1c** (Figure 1b), the adamantylthio units are located on the same face of the perylene diimide core, whereas in the 1,6-derivative, **2c**, adamantylthio units are arranged on opposing faces of the perylene diimide core (Figure 1c). The relative orientation of the bay region substituents leads to different stacking behavior of the compounds, as discussed for each individual case.

Compound **1a** crystallizes in the triclinic space group *P*-1, with two perylene diimide molecules and a diethyl ether molecule in the unit cell. A twisted arrangement of the perylene diimide core was observed, such that the perylene core can be considered as two naphthyl moieties linked at the 13/14 and 17/18 positions (see Figure S22, Supporting Information, for the numbering scheme). An interplanar angle of 25.7° was observed between these two subunits, within the range of angles typically observed for other disubstituted perylene diimide derivatives.[8a] The twisting of the perylene core of **1a** is accompanied by relatively long internaphthyl C−C bond lengths, 1.475−1.486 Å, by comparison with average C═C

dx.doi.org/10.1021/jo400026r | J. Org. Chem. 2013, 78, 2853−2862

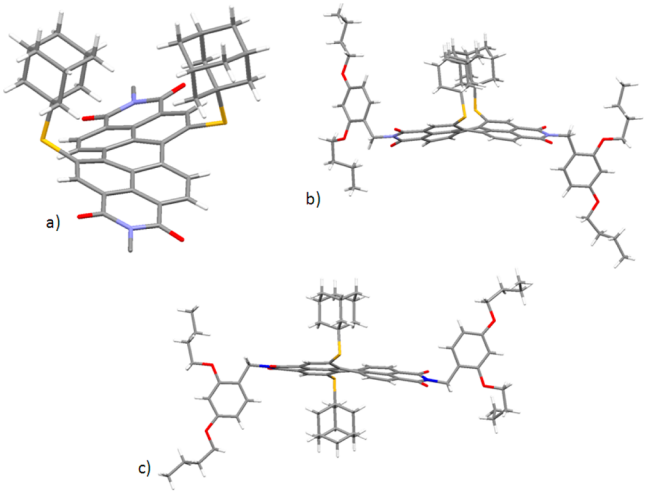

Figure 1. View of the single crystal structures of (a) **1a** showing a twisted arrangement of one of the perylene cores of the molecule (the second perylene diimide derivative in the asymmetric unit, solvent molecule and parts of the imide butyl substituent, are omitted for clarity); (b) structure of **1c** showing the orientation of the adamantylthio substituents on the same face of the PTCDI core; (c) structure of **2c** showing the orientation of the adamantylthio substituents on opposing faces of the PTCDI core.

bond lengths of 1.407 Å for the naphthyl moieties of the molecule. The adamantyl moieties are positioned on the same side of the PTCDI plane with the opposing side of each molecule participating in $\pi-\pi$ interactions leading to the formation of cofacial dimers of two molecules of **1a** (Figure 2a). The cofacial dimers are packed such that the adamantyl and butyl groups on adjacent molecules adopt positions in close proximity (Figure S1, Supporting Information).

Compounds **1c** and **2c** both crystallize in the monoclinic space group $P2_1/c$, each with one PTCDI molecule in the unit cell. As with **1a**, both **1c** and **2c** adopt a twisted arrangement of the perylene diimide core. The interplanar angles between the two napthyl subunits of the perylene core of **1c** (27.47°) and **2c** (18.50°) were observed. The perylene twisting is accompanied by lengthening of the internaphthyl C−C bonds to 1.469(8)/1.478(8) Å (**1c**) and 1.452(7)/1.466(7) Å (**2c**), as compared to average bond lengths in the naphthyl moieties of 1.400 and 1.407 Å, respectively. The smaller internaphthyl twist angle observed for **2c**, in comparison to both **1c** and **1a**, is surprising and inspection of bond lengths and angles does not reveal clear evidence for the more planar arrangement of the 1,6-isomer. Indeed, both C−S−C angles and C−S bond lengths are very similar for the three compounds. The only clear distinction between **1a**, **1c**, and **2c** is the orientation of the adamantyl groups in the 1,6-isomer **2c** with these substituents positioned on opposing faces of the perylene core in contrast to the arrangement seen for the two 1,7-isomers **1a** and **1c**. It is conceivable that this alternative arrangement allows the alternative packing arrangement described below and a flattening of the perylene core in **2c**.

As mentioned above, the adamantyl moieties in **2c** are positioned on opposing sides of the PTCDI plane (Figure 1c), leading to a dimeric arrangement of the molecules (Figure 2b). The shortest centroid to centroid distances are of more than 4 Å, indicating the absence of significant $\pi-\pi$ interactions between adjacent molecules, presumably as a result of the large steric bulk of both the adamantyl and DBOB imide substituents (Figure S2, Supporting Information). In contrast, in the structure of **1c** adjacent molecules within dimers adopt a

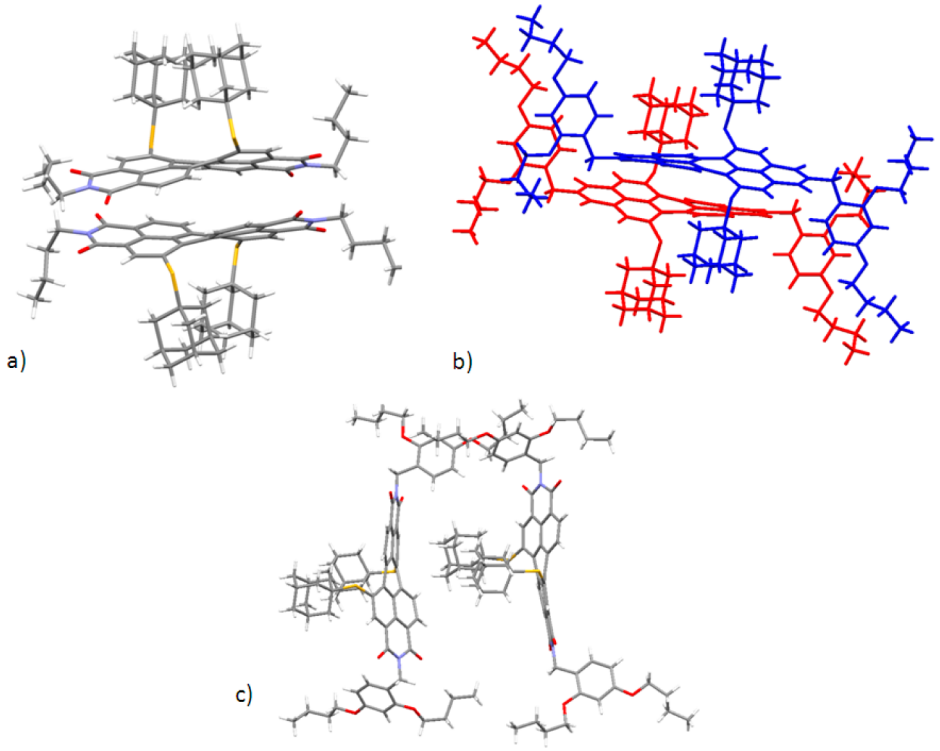

Figure 2. Views of (a) cofacial pairs of molecules of **1a** where each pair comprises the same atropo-enantiomers, either *MM*- and *PP*-dimers; (b) dimeric arrangement adopted by **2c**; (c) orientation of adjacent molecules of **1c** showing that $\pi-\pi$ interactions are precluded in this structure.

dx.doi.org/10.1021/jo400026r | *J. Org. Chem.* 2013, 78, 2853−2862

side-on arrangement with the closest contact occurring between the thioether sulfur atom and an imide nitrogen of the opposing molecule (N···S = 3.20 Å); the exposed face of each PTCDI unit is in closest proximity to an adamantyl group from the adjacent molecule (Figure 2c).

Disubstituted PTCDI derivatives can exhibit inherent chirality due to twisting of the aromatic perylene core leading to both *M* and *P* atropo-enantiomers.[20] For the compounds in this study it would be anticipated that interconversion of the isomers would be facile at room temperature,[20] and thus it is not surprising that the compounds crystallize in centrosymmetric space groups and thus do not exhibit overall chirality. The structure of **1a** contains pairs of molecules which contain exclusively one isomer, either *M* or *P*, and so the structure is built from alternating pairs of *MM*- and *PP*-dimers.[21]

The bond lengths and twist angles of the crystal structures obtained were compared to the structures generated by gas-phase geometry optimization calculations on model structures; this indicated that the perylene diimide cores of the modeled structures of **1a** and **2a** were in close agreement with those of the experimentally determined structures of **1a** and **2c** (Table S2, Supporting Information).

Electrochemical and Spectroscopic Investigations. Cyclic voltammetry (CV) and IR/UV/vis/EPR spectroscopic measurements were performed on compounds **1a**−**c** and **2a**−**c** and their corresponding electrochemically generated reduced states; these measurements were compared, where appropriate, to measurements made on a diSPr-PTCDI substituted derivative, **3**. CV experiments on each of the compounds show two reduction processes in the range −0.94 to −1.22 V and oxidation processes in the range +0.94 to +1.20 V (Figure 3, Table 1). The reductions follow trends reported for other

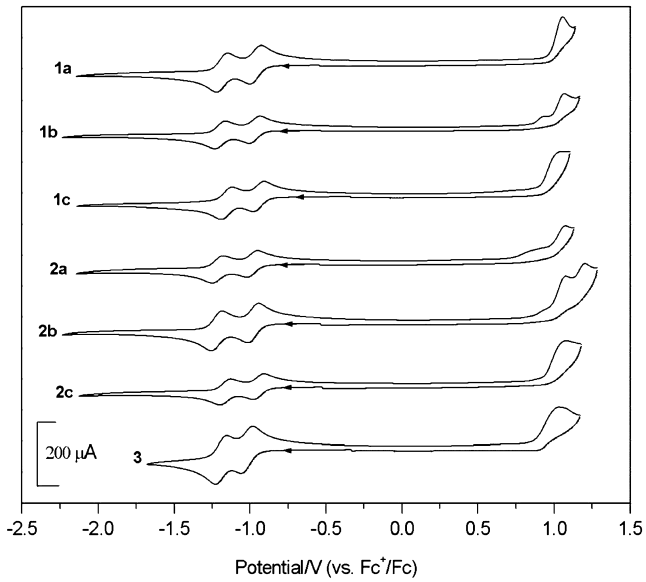

Figure 3. View of cyclic voltammograms recorded for **1**(**a**−**c**), **2**(**a**−**c**), and **3** in CH_2Cl_2 containing $[Bu_4N][BF_4]$ (0.4 M) at 0.1 V s^{-1}.

perylene diimide compounds.[8] Hence, all the compounds undergo two one-electron reduction processes, based on the perylene diimide core, that are reversible. The potentials for the reductions of **1a**−**c** and **2a**−**c** are consistent with less electron density on the perylene core when compared to analogous N-substituted complexes.[8b,15] Variation in reduction potentials is

Table 1. Cyclic Voltammetry Data[a]

	first reduction	second reduction	oxidations	$\Delta E(Fc^+/Fc)$
1a	−0.96 (0.07)	−1.18 (0.07)	1.05	(0.07)
1b	−0.97 (0.07)	−1.20 (0.07)	0.94, 1.07	(0.07)
1c	−0.94 (0.07)	−1.15 (0.08)	1.04	(0.07)
2a	−0.96 (0.07)	−1.22 (0.08)	1.07	(0.07)
2b	−0.98 (0.07)	−1.22 (0.07)	1.08, 1.20	(0.08)
2c	−0.95 (0.07)	−1.17 (0.07)	1.07	(0.07)
3	−1.02 (0.08)	−1.19 (0.07)	1.03	(0.07)

[a]All potentials reported as $E_{1/2}$ (= $(E_p^a + E_p^c)/2$) in V vs Fc^+/Fc at 0.1 Vs^{-1} scan rate and quoted to the nearest 0.01 V. Values in parentheses are ΔE (= $E_p^a - E_p^c$) for the couple at 0.01 Vs^{-1}. All cyclic voltammetry measurements were performed on CH_2Cl_2 solutions of the relevant compounds with 0.4 M in $[NBu_4][BF_4]$ as supporting electrolyte.

small across the series, but trends were observed by cyclic voltammetry and confirmed by square wave voltammetry (Figure S4, Supporting Information, Table 1, and Table S1, Supporting Information). First, there is a small influence on $E_{1/2}$ values with the nature of the imide substituent. This is noted in each series **1a** (−0.96 V), **1b** (−0.97 V), and **1c** (−0.94 V) and similarly for **2a** (−0.96 V), **2b** (−0.98 V), and **2c** (−0.95 V) where the presence of benzyl substitution at the imide results in slightly lower energy reductions suggesting less electron density in the perylene core in these cases. Second, there is a larger influence on $E_{1/2}$ with variation in the bay substituent from *S*-adamantyl to *S*-propyl, **1a** (−0.96 V) vs **3** (−1.02 V). Third, there is a small difference between the 1,6 and 1,7 forms, best distinguished in the potential of the second reduction, with the 1,6 isomers reducing at potentials slightly more negative than their 1,7 analogues. This is consistent with previous studies of other pairs of 1,6 and 1,7 isomers of disubstituted perylene-diimides.[8a,b,14] The irreversible oxidation processes are commonly observed for PTCDI derivatives and were not studied further.

Of interest is the difference in potentials between the first and second reductions for each molecule (Table 1). This difference results from Coulombic repulsion between the added electrons acting through the π-framework of the aromatic core and is dependent upon the resonance energy and the ability of the core to delocalize the first electron density.[22] In the case of adamantylthio-substituted species there is a significantly larger separation between the two reductions (0.21 − 0.26 V) compared to the propylthio-substituted compound **3** (0.17 V). One explanation might be that, in solution, the bulky adamantyl substituents induce larger twisting in the perylene core, perturbing effective delocalization of electron density. In the absence of a crystallographic study of **3** this cannot be confirmed and it should be borne in mind that **3** is a mixture of 1,6- and 1,7 isomers. Given these small differences between the 1,7 and 1,6 forms it would be difficult to distinguish between the two forms, or mixtures thereof, by means of cyclic voltammetry.

The in situ one- and two-electron reductions of **1**−**3** were followed by UV/vis spectroelectrochemistry at an optically transparent electrode. Spectroelectrochemical studies demonstrate that in the range 400−900 nm the spectral profile for each series (**1a**−**c** and **2a**−**c**) is essentially the same at each redox level studied; see Figure 4 for a representative example and the Supporting Information for all other cases and a table of data. The one-electron reduced radical anions show major

dx.doi.org/10.1021/jo400026r | J. Org. Chem. 2013, 78, 2853−2862

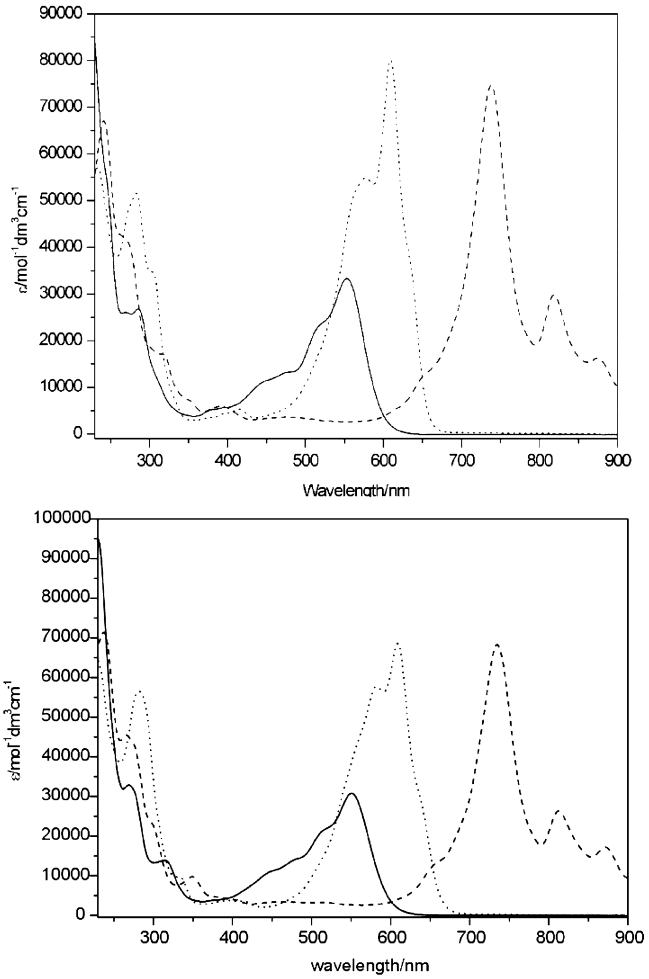

Figure 4. View of UV−vis spectra recorded in CH_2Cl_2 containing $[Bu_4N][BF_4]$ (0.4 M) using spectroelectrochemical methods for **1a** (top) and **2a** (bottom) at 273 K. The spectra of **1a**/**2a** are represented by the solid line, $\mathbf{1a}^-/\mathbf{2a}^-$ (dashed line), $\mathbf{1a}^{2-}/\mathbf{2a}^{2-}$ (dotted line).

bands red-shifted relative to their parent molecules, with series of transitions extending into the nIR region. It is noted that for the monoanions, while the spectral profiles are similar there is a slight red shift for **1** versus **2** in bands >700 nm. The second reduction blue-shifts the spectra with respect to those of the radical anion, with the most intense transition for **1b** (611 nm), **1c** (609 nm) and **1a** (609 nm); **2b** (610 nm), **2c** (609 nm), **2a** (609 nm), **3** (624 nm) all occurring at similar wavelength, a result consistent with other diimide perylene compounds (see the Supporting Information for data).

TD-DFT calculations were performed on the neutral, mono-, and direduced species of **1a** and **2a** in order to provide insight into the nature of the transitions that dominate in the experimental spectra. The results are summarized in the Supporting Information. A reasonable agreement with experimental data was seen in calculations of the neutral state. Calculations of the mono- and direduced states reflect the trend seen in the experimental data of major bands being red-shifted on reduction of the parent molecules, then blue-shifted on reduction to the direduced state. However, a close agreement with peak shifts was not seen, particularly in the case of the direduced states. Improvements in the calculations were attempted by altering the solvation model, the dielectric constant and the basis set, but a closer agreement was not obtained.

The electrochemical one-electron reduction of each compound gave species that were paramagnetic. For fluid solutions, at ambient temperature, EPR spectroscopy gave signals consistent with generation of the radical anions (see Figure 5

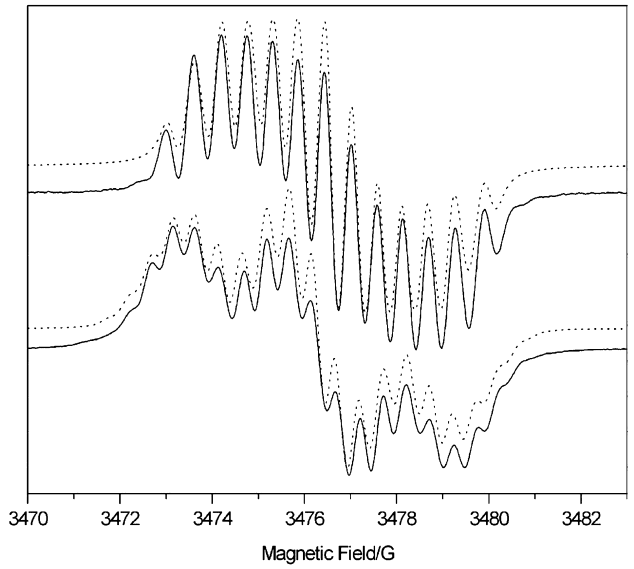

Figure 5. Experimental (solid line) and simulated (dotted) EPR spectra of (top) electrochemically generated $\mathbf{1a}^-$ and (bottom) $\mathbf{2a}^-$ in CH_2Cl_2 containing $[Bu_4N][BF_4]$ (0.4 M) at 291 K.

and the Supporting Information for spectra). Two-electron reduction of **1**−**3** yields the dianions, all of which are dark blue. These solutions were essentially EPR silent, with reduced signals relative to their monoanion analogues (between 1 and 16% of the intensity of the anion spectrum as determined by double integration).

For the monoreduced species the shape of the EPR spectrum appears to distinguish between 1,6- and 1,7-substituted species. For most of these spectra we have produced reasonable simulations of the experimental data and the parameters used for these simulations are listed in Table 2.

DFT calculations were carried out for compounds $[\mathbf{1a}]^-$ and $[\mathbf{2a}]^-$ in order to generate theoretical hyperfine coupling constants. Trends obtained from theoretical calculations for the hyperfine coupling constants around the perylene core are in reasonable agreement with those determined from the simulation of experimental data and allow some insight into the distribution of electron density in these anions. These results suggest that for $[\mathbf{1b}]^-$, unpaired spin density is distributed centrosymmetrically about the perylene core[15b] and that the hydrogen hyperfine coupling constants that dominate the experimental spectrum derive largely from the (6,12) (a_{2H} 1.50 × 10^{-4} cm^{-1}) and (5,11) (a_{2H} 0.68 × 10^{-4} cm^{-1}) positions, with only a small contribution (a_{2H} 0.08 × 10^{-4} cm^{-1}) from the (2,8) position. Significant electron density resides on the N and O atoms of the diimide groups, the former contributing to the experimental spectrum. For $[\mathbf{2b}]^-$ the largest distribution of spin density is localized at the (7,12) (a_{2H} 1.93 × 10^{-4} cm^{-1}) position in the half of the perylene core unsubstituted by the adamantylthio groups; lesser contributions from the (2,5) (a_{2H} 0.54 × 10^{-4} cm^{-1}) and (8,11) (a_{2H} 0.50 × 10^{-4} cm^{-1}) positions, together with contributions from the

dx.doi.org/10.1021/jo400026r | J. Org. Chem. 2013, 78, 2853−2862

Table 2. Experimental EPR Data for Monoanionic Species

compd	g_{iso}	a_{iso} ($\times 10^{-4}$ cm^{-1})[b]	linewidth (G)
$\mathbf{1a}^{1-}$	2.0032	1.50 (a_{2H}), 0.68 (a_{2H}), 0.08 (a_{2H}), 0.51 (a_{2N})	0.27[c]
$\mathbf{1b}^{1-}$	2.0034	1.52 (a_{2H}), 0.68 (a_{2H}), 0.08 (a_{2H}), 0.51 (a_{2N})	0.29[c]
$\mathbf{1c}^{1-}$	2.0034		
$\mathbf{2a}^{1-}$	2.0032	1.94 (a_{2H}), 0.54 (a_{2H}), 0.50 (a_{2H}), 0.40 (a_{2N}), 0.37 (a_{4H})	0.40[d]
$\mathbf{2b}^{1-}$	2.0032	1.93 (a_{2H}), 0.54 (a_{2H}), 0.50 (a_{2H}), 0.40 (a_{2N}), 0.37 (a_{4H})	0.44
$\mathbf{2c}^{1-}$	2.0034	1.93 (a_{2H}), 0.51 (a_{4H}), 0.42 (a_{2N}), 0.39 (a_{4H})	0.41
$\mathbf{3}^{1-}$	2.0034	[e]	

[a]In CH_2Cl_2 containing [^{n}Bu$_4$N][BF$_4$] (0.4 M) at 298 K. [b]Simulation of experimental parameters using Gaussian line shape unless stated otherwise. [c]Lorentzian line shape. [d]80:20 Guassian/Lorentzian line shape. [e]Insufficient resolution.

diimide nitrogens give a distribution of electron density that is symmetric along the N − N axis of the molecule. Calculated spin density diagrams of [**1a**]$^-$ and [**2a**]$^-$ (Figure 6) and

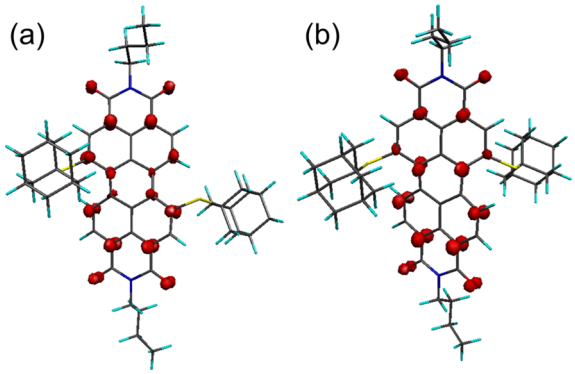

Figure 6. Total spin density shown in red for models of (a) [**1a**]$^-$ and (b) [**2a**]$^-$ derived from DFT calculations.

indicate a difference in spin density distribution between the case of **1a**, which contains two monosubstituted naphthalene subunits, and **2a**, which contains one unsubstituted and one disubstituted naphthalene subunit. We speculate that this difference gives rise to the observed differences in the experimental EPR spectra.

IR spectra of the neutral, monoreduced, and direduced species of **1b** and **2b** were recorded (Figure 7) and calculated (Table 3) and are presented in the range between 1725 and 1500 cm^{-1}; experimental bands to lower energy are obscured by the limits of solvent and [^{n}Bu$_4$N][BF$_4$] electrolyte. In this region the IR spectra of **1b** and **2b** are very similar and consist of three distinct bands. The bands at 1696 and 1658 cm^{-1} are invariant between 1,7 and 1,6-forms and are assigned as the symmetric and asymmetric vibrations of the imide carbonyls, respectively.[23] The band at ca. 1585 cm^{-1} is assigned to stretching modes in the carbon framework of the perylene core the overall effect of which appears as a wag of the C−H bonds;[24] this band appears to be structured for **1b**.[16] These assignments are consistent with the results of our DFT calculations which reproduce the experimental spectrum well after the requisite scaling of energies.[25] Reduction to the monoanionic forms, [**1b**]$^-$ and [**2b**]$^-$, depletes bands associated with their respective neutral species and results in more complex spectra; ν(CO) bands are shifted to lower energy relative to their neutral analogues and this is consistent with results found for previously reported and related naphthalene diimide derivatives.[26] Theory predicts this change, although the reproduction of absolute energies is poorer than for the neutral forms. It is noted that bands assigned to ν(CO) are almost identical for [**1b**]$^-$ and [**2b**]$^-$, reflecting a similarity in local environment and consistent with the model proposed by Lee et al.[22] in which the electron density resides primarily on the carbonyl oxygens; however, those bands assigned to ν(CC) differ significantly in position and intensity indicating the sensitivity of these environments to the different isomeric forms upon reduction.

For [**2b**]$^-$, where the perylene core can be considered as a composite of two different naphthalene subunits, one substituted by two adamantanethiol groups, the bands at 1581 and 1566 cm^{-1} are assigned to an in-plane C−H wag motion in the unsubstituted and substituted naphthalene groups, respectively. For the unsubstituted naphthalene core the band at 1581 cm^{-1} appears as a symmetric wag while the band at 1532 cm^{-1} is the corresponding asymmetric motion. Conversion of anion to dianion further shifts all bands to lower energy, with the corresponding depletion of bands associated with the monoanions. Theory has predicted the same ordering of bands in the dianionic species ie. ν_{sym}(CO) > ν_{asym}(CO) > ν(CC); however, the shift of ν(CO) to lower energy relative to the anionic forms results in possible overlap with ν(CC) making unambiguous assignment of the experimental bands difficult.

CONCLUSIONS

A combination of electrochemical and spectroscopic methods, complemented by theoretical calculations, has provided a framework by which the effect of mono- and direductions in a series of 1,6- and 1,7-isomers of diadamantanethio-substituted PTCDI species can be monitored and understood. Experimental EPR results for the monoanions are consistent with previous studies of PTCDIs and show unpaired electron density based around the perylene core, with a contribution from the diimide nitrogens. However, the contribution from the diimide carbonyls is not reported by this spectroscopic technique due to the low natural abundance of spin active nuclei. Infrared spectroscopy of the monoanions highlights this shortfall and shows that reduction has an effect both in the carbon framework of the perylene core, as observed as shifts in ν(CC) bands, and at the diimide carbonyls. The IR spectra of **1b** and **2b** are almost indistinguishable, in our limited spectral window, as the neutral species and this similarity extends to the ν(CO) bands for the monoanionic forms. The relatively small shift in ν(CO) bands on first reduction (*ca.* 50 cm^{-1}) and the presence of a single environment for each of the symmetric/asymmetric stretches indicates delocalization between all carbonyl positions in these anions. This view of highly delocalized anions is confirmed by theory. Plots of total spin density for the anions show a centrosymmetric distribution for 1,7-substituted **1a.** For 1,6-substituted **2b**, containing mirror

dx.doi.org/10.1021/jo400026r | J. Org. Chem. 2013, 78, 2853−2862

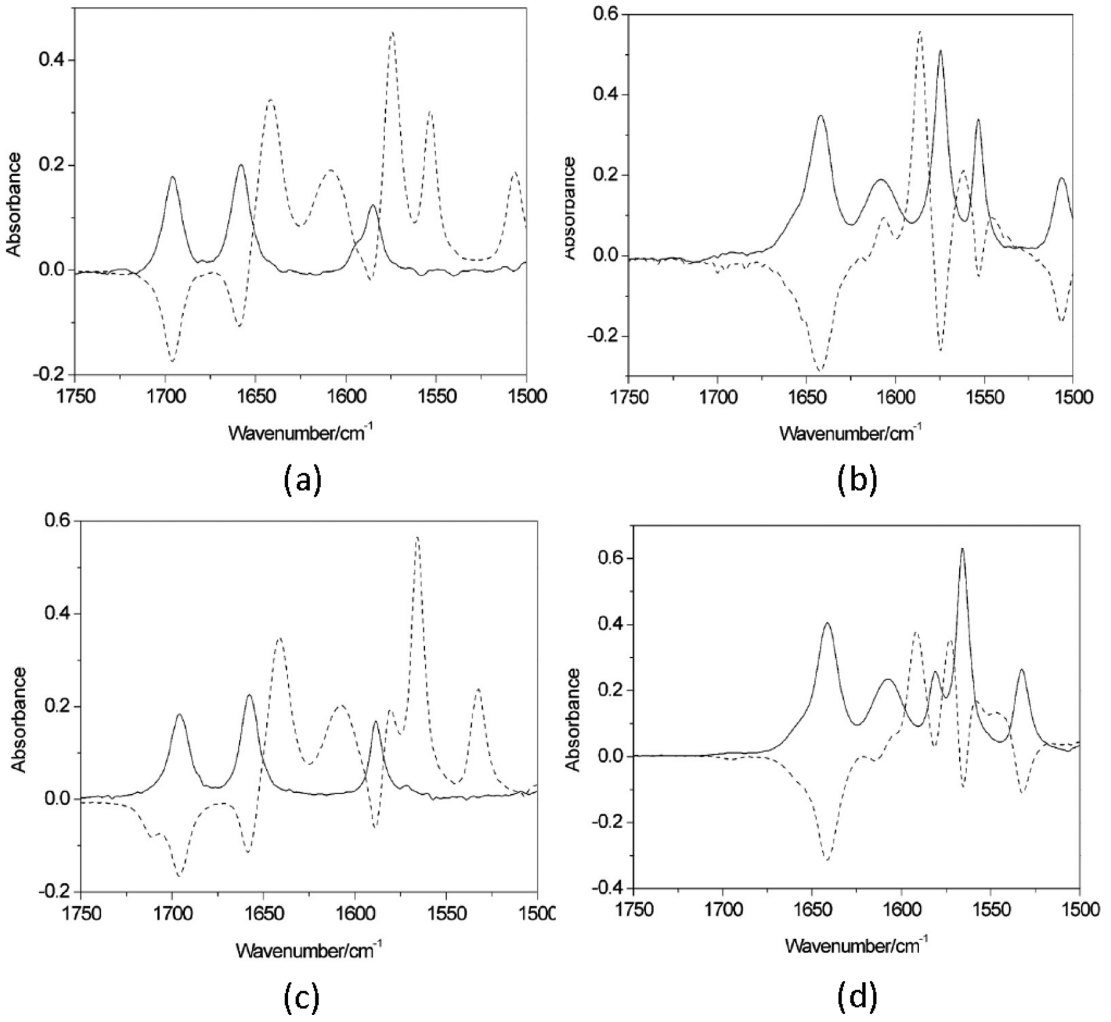

Figure 7. Views of IR spectra for (a) **1b** (solid line) and following electrochemical reduction (dashed line) of **1b** (bleached bands) to $\mathbf{1b}^-$ (positive absorbances); (b) $\mathbf{1b}^-$ (solid line) and following electrochemical reduction (dashed line) of $\mathbf{1b}^-$ (bleached bands) to $\mathbf{1b}^{2-}$ (positive absorbances); (c) **2b** (solid line) and following electrochemical reduction (dashed line) of **2b** (bleached bands) to $\mathbf{2b}^-$ (positive absorbances); (b) $\mathbf{2b}^-$ (solid line) and following electrochemical reduction (dashed line) of $\mathbf{2b}^-$ (bleached bands) to $\mathbf{2b}^{2-}$ (positive absorbances). All spectra recorded in CH_2Cl_2 containing $[Bu_4N][BF_4]$ (0.4 M) in the range 1500−1750 cm^{-1}.

Table 3. IR Spectroscopic Data Recorded for 1b and 2b over the Range 1500−1750 cm^{-1}

	1b			2b		
	experiment (cm^{-1})	theory (cm^{-1})	assignment	experiment (cm^{-1})	theory (cm^{-1})	assignment
neutral	1696	1699	$\nu(CO)_{sym}$	1696	1700	$\nu(CO)_{sym}$
	1658	1666	$\nu(CO)_{asym}$	1658	1667	$\nu(CO)_{asym}$
	1585	1570	$\nu(CC)_{perylene}$	1589	1569	$\nu(CC)_{perylene}$
monoanion	1642	1658	$\nu(CO)_{sym}$	1642	1659	$\nu(CO)_{sym}$
	1608	1628	$\nu(CO)_{asym}$	1608	1629	$\nu(CO)_{asym}$
	1575	1561	$\nu(CC)_{perylene}$	1581	1551	$\nu(CC)_{perylene}$
	1553	1528	$\nu(CC)_{perylene}$	1566	1520	$\nu(CC)_{perylene}$
	1506	1489	$\nu(CC)_{perylene}$	1532	1467	$\nu(CC)_{perylene}$
Dianion	1606	1630	$\nu(CO)_{sym}$	1592	1628	$\nu(CO)_{sym}$
	1586	1582	$\nu(CO)_{asym}$	1573	1581	$\nu(CO)_{asym}$
	1562,1545	1522, 1487	$\nu(CC)_{perylene}$	1559,1546	1555,1502	$\nu(CC)_{perylene}$

symmetry along the PTCDI framework, greater spin density is distributed in the unsubstituted naphthalene subunit of the perylene core. The second reduction to the dianion further shifts both ν(CO) and ν(CC) bands to lower energy again indicating that the additional electron density resides both on the diimide groups and the core perylene; these species are diamagnetic at ambient temperature, indicating strong coupling between the two added electrons but negating the use of EPR spectroscopy to probe this redox level. The UV−vis spectra of these dianions show a remarkable similarity of band position for the lowest energy transition, suggesting direduction generates a chromophore common to both 1,7 and 1,6 forms, and it is

dx.doi.org/10.1021/jo400026r | J. Org. Chem. 2013, 78, 2853−2862

convenient to consider that this CT transition occurs between orbitals with increased quinoidal character.

The use of spectroelectrochemical methods, both UV−vis and IR spectroscopic measurements, for probing the reduced states of PTCDI derivatives facilitates a greater understanding of the nature of these reduced states furthering our understanding of these important species for molecular electronics and optical applications.

EXPERIMENTAL SECTION

Synthetic Procedures. Compound **1b** was prepared according to our previously reported procedure.[18] Details of characterization are reported here for comparison.

*Compounds **1** and **2**: General Procedure.* A 250 mL round-bottomed flask was flame-dried, backfilled with nitrogen three times, and charged with dry toluene (100 mL). A mixture of 1,6- and 1,7-isomers of *N*,*N*′-bis(alkyl)dibromo-3,4:9,10-perylenetetracarboxylic diimide and 1-adamantanethiol (3 equiv) was added, and the mixture was heated at 80 °C under N_2 for 1 h. ^{t}BuONa (6 equiv) and $Pd(PPh_3)_4$ (5 mol %) were then added, and the mixture was heated at 90 °C under N_2 overnight. The toluene was then removed in vacuo, and the resulting purple residue was dissolved in chloroform and filtered by gravity before being washed with water. The organic fractions were dried over Na_2SO_4, filtered by gravity, and evaporated in vacuo to yield a dark purple solid, which was purified via column chromatography (SiO_2, $CHCl_3$).

***1a** (1,7 isomer):* R_f = 0.29 (64 mg, 51%); ^{1}H NMR (400 MHz, $CDCl_3$) δ_H = 9.43 (d, *J* = 8.03 Hz, 2 H) 8.91 (s, 2 H) 8.68 (d, *J* = 8.03 Hz, 2 H) 4.23 (d, *J* = 7.65 Hz, 4 H) 1.73−1.90 (m, 13 H) 1.57−1.65 (m, 28 H) 1.51 (d, *J* = 14.68 Hz, 8 H) 1.34−1.46 (m, 7 H) 1.23−1.31 (m, 2 H) 1.04 (t, *J* = 7.34 Hz, 6 H); ^{13}C NMR (126 MHz, $CDCl_3$) δ_C = 163.5, 163.4, 141.6, 139.4, 134.1, 132.0, 130.6, 129.8, 128.3, 127.3, 122.6, 120.5, 53.5, 43.4, 40.5, 35.8, 30.3, 30.0, 20.5, 13.9; MS (MALDI-TOF) *m*/*z* 834.4 (M). Anal. Calcd for $C_{52}H_{54}N_2O_4S_2$: C, 74.79; H, 6.52; N, 3.35. Found: C, 74.88; H, 6.47; N 3.25.

***2a** (1,6 isomer):* R_f = 0.44 (14 mg, 11%); ^{1}H NMR (400 MHz, $CDCl_3$) δ ppm 9.52 (d, *J* = 8.03 Hz, 2 H) 8.97 (s, 2 H) 8.72 (d, *J* = 8.03 Hz, 2 H) 4.09−4.43 (m, 4 H) 2.08 (br s, 7 H) 1.90−1.98 (m, 2 H) 1.84 (d, *J* = 2.76 Hz, 20 H) 1.69 (br s, 14 H) 1.63 (d, *J* = 2.13 Hz, 14 H) 1.41−1.55 (m, 19 H) 1.28 (s, 15 H) 1.04 (d, *J* = 0.88 Hz, 6 H); ^{13}C NMR (126 MHz, $CDCl_3$) δ_C = 168.8, 163.3, 141.6, 139.3, 133.3, 132.0, 131.8, 129.2, 129.2, 127.8, 127.3, 127.0, 122.9, 120.2, 53.9, 43.5, 40.6, 40.5, 35.8, 30.3, 30.2, 30.0, 20.5, 20.5, 13.9, 13.8; MS (MALDI-TOF) *m*/*z* 834.4 (M). Anal. Calcd for $C_{52}H_{54}N_2O_4S_2$: C, 74.79; H, 6.52; N, 3.35. Found: C, 74.70; H, 6.58; N 3.30.

***1b** (1,7 isomer):* 339 mg, 55%; ^{1}H NMR (400 MHz, $CDCl_3$) δ_H = 9.42 (d, *J* = 8.03 Hz, 2 H) 8.93 (s, 2 H) 8.68 (d, *J* = 8.16 Hz, 2 H) 4.07−4.27 (m, 4 H) 2.08 (br s) 1.84 (m) 1.22−1.74 (m) 0.99 (t, *J* = 7.40 Hz, 6 H) 0.91 (t, *J* = 7.03 Hz, 6 H); ^{13}C NMR (126 MHz, $CDCl_3$) δ_C = 163.9, 163.8, 141.5, 139.3, 134.1, 131.9, 130.8, 129.9, 128.4, 127.3, 122.6, 120.5, 53.5, 44.4, 43.5, 38.0, 35.8, 30.7, 30.1, 28.7, 24.1, 23.1, 14.1, 10.6; MS (MALDI-TOF) *m*/*z* 946.5 (M). Anal. Calcd for $C_{60}H_{70}N_2O_4S_2$: C, 76.07; H, 7.45; N, 2.96. Found: C, 75.97; H, 7.54; N 2.88.

***2b** (1,6 isomer):* R_f = 0.68 (86 mg, 14%); ^{1}H NMR (400 MHz, $CDCl_3$) δ_H = 9.51 (d, *J* = 8.03 Hz, 2 H) 8.98 (s, 2 H) 8.72 (d, *J* = 8.03 Hz, 2 H) 4.08−4.33 (m, 4 H) 2.34 (br s) 1.94−2.11 (m) 1.87 (br s) 1.23−1.72 (m) 0.99 (t, *J* = 7.40 Hz, 6 H) 0.84−0.95 (m, 6 H); ^{13}C NMR (126 MHz, $CDCl_3$) δ_C = 164.2, 163.7, 141.6, 139.2, 133.3, 132.0, 132.9, 129.3, 129.2, 127.9, 127.3, 127.0, 122.9, 120.2, 54.0, 44.5, 44.4, 43.5, 38.1, 38.0, 35.8, 30.8, 30.7, 30.0, 28.8, 28.6, 24.2, 24.1, 23.1, 14.1, 14.1, 10.7, 10.6; MS (MALDI-TOF) *m*/*z* 946.5 (M). Anal. Calcd for $C_{60}H_{70}N_2O_4S_2$: C, 76.07; H, 7.45; N, 2.96. Found: C, 76.17; H, 7.37; N 3.00.

***1c** (1,7 isomer):* R_f = 0.32 (329 mg, 46%); ^{1}H NMR (400 MHz, $CDCl_3$) δ_H = 9.44 (d, *J* = 8.16 Hz, 2 H) 8.92 (s, 2 H) 8.68 (d, *J* = 8.16 Hz, 2 H) 7.17 (d, *J* = 8.41 Hz, 2 H) 6.47 (s, 2 H) 6.41 (d, *J* = 6.53 Hz, 2 H) 5.42 (s, 3 H) 4.00 (t, *J* = 6.40 Hz, 4 H) 3.93 (t, *J* = 6.53 Hz, 4 H) 1.68−1.89 (m, 13 H) 1.31−1.64 (m, 47 H) 0.97 (q, 12 H); ^{13}C NMR (126 MHz, $CDCl_3$) δ_C = 163.5, 159.6, 157.8, 141.7, 139.4, 134.2, 131.9, 130.6, 129.9, 129.1, 128.4, 127.4, 122.7, 120.7, 117.1, 104.5, 99.7, 67.9, 67.7, 53.4, 43.4, 39.3, 35.8, 31.4, 31.3, 30.0, 19.4, 19.2, 14.0, 13.8; (MALDI-TOF) *m*/*z* 1190.6 (M). Anal. Calcd for $C_{74}H_{82}N_2O_8S_2$: C, 74.59; H, 6.94; N, 2.35. Found: C, 74.68; H, 6.94; N 2.35.

***2c** (1,6 isomer):* R_f = 0.50 (86 mg, 12%); ^{1}H NMR (400 MHz, $CDCl_3$) δ_H = 9.54 (d, *J* = 8.03 Hz, 2 H) 8.97 (s, 2 H) 8.72 (d, *J* = 8.03 Hz, 2 H) 7.17 (dd, *J* = 18.82, 8.41 Hz, 2 H) 6.31−6.57 (m, 4 H) 5.43 (d, *J* = 8.78 Hz, 4 H) 3.84−4.11 (m, 8 H) 1.66−1.98 (m, 16 H) 0.70−1.56 (m, 48 H); ^{13}C NMR (126 MHz, $CDCl_3$) δ_C = 163.7, 163.2, 159.6, 159.6, 157.8, 157.8, 141.9, 139.7, 133.3, 131.9, 131.7, 129.3, 129.3, 128.9, 127.9, 127.3, 127.2, 123.1, 120.4, 117.2, 117.0, 104.5, 10.5, 99.7, 67.9, 67.9, 67.7, 53.9, 43.4, 39.4, 39.3, 35.8, 31.4, 31.3, 31.3, 30.0, 19.4, 19.4, 19.2, 14.0, 13.8; MS (MALDI-TOF) *m*/*z* 1190.6 (M). Anal. Calcd for $C_{74}H_{82}N_2O_8S_2$: C, 74.59; H, 6.94; N, 2.35. Found: C, 74.45; H, 6.95; N 2.32.

Compound **3**, an inseparable 1:4 mixture of 1,6- and 1,7-isomers of *N*,*N*′-bis(*n*-butyl)dipropanethio-3,4:9,10-perylenetetracarboxylic acid diimides, was prepared according to a previously published route.[7f]

Single-Crystal X-ray Diffraction Structural Studies. Single-crystal diffraction data on **1a** were collected at 150(2)K on a Bruker SMART APEX CCD area detector diffractometer using graphite-monochromated Mo Kα radiation. Data for **1c** and **2c** were collected at 90(2) K on an Oxford Diffraction SuperNova area detector diffractometer using mirror-monochromated Cu Kα radiation. Further details of structure refinement can be found in the Supporting Information.

Electrochemical and Optical Spectroscopy Investigations. Dichloromethane (Fisher) was freshly distilled under an atmosphere of dinitrogen from calcium hydride. Ferrocene was used as received. $[NBu_4][BF_4]$ was prepared by literature methods.[27] Cyclic voltammetric and coulometric studies were carried out using an Autolab PGSTAT20 potentiostat. Standard cyclic voltammetry was carried out under an atmosphere of argon using a three-electrode arrangement in a single compartment cell. A glassy carbon working electrode, a Pt wire secondary electrode, and a saturated calomel reference electrode, chemically isolated from the test solution via a bridge tube containing electrolyte solution and fitted with a porous Vycor frit, were used in the cell. The solutions were 10^{-3} M in test compound and 0.4 M in $[NBu_4][BF_4]$ as supporting electrolyte. Redox potentials are quoted versus the ferrocenium-ferrocene couple used as an internal reference.[28] Compensation for internal resistance was not applied.

Bulk electrolysis experiments, at a controlled potential, were carried out using a two-compartment cell. The Pt/Rh gauze basket working electrode was separated from the wound Pt/Rh gauze secondary electrode by a glass frit. A saturated calomel reference electrode was bridged to the test solution through a Vycor frit oriented at the center of the working electrode. The working electrode compartment was fitted with a magnetic stirrer bar, and the test solution was stirred rapidly during electrolysis. Solutions were 0.4 M in $[NBu_4][BF_4]$ as supporting electrolyte and 10^{-3} M in test compound and were prepared using Schlenk line techniques. Electrolysed solutions were transferred to quartz tubes, via Teflon canula, for analysis by EPR spectroscopy. EPR spectra were recorded on a Bruker EMX spectrometer and simulated using WINEPR SimFonia, Shareware version 1.25, Brüker Analytische Messtechnik GmbH.

UV/vis spectroelectrochemical experiments were carried out with an optically transparent electrochemical (OTE) cell (modified quartz cuvette, optical path length: 0.5 mm).[29] A three-electrode configuration, consisting of a Pt/Rh gauze working electrode, a Pt wire secondary electrode (in a fritted PTFE sleeve) and a saturated calomel electrode, chemically isolated from the test solution via bridge tube containing electrolyte solution and terminated in a porous frit, was used in the cell. The potential at the working electrode was controlled by a Sycopel Scientific Ltd. DD10 M potentiostat. The UV/vis spectra were recorded on a Perkin-Elmer Lambda 16 spectrophotometer. The cavity was purged with dinitrogen, and temperature control at the sample was achieved by flowing cooled dinitrogen across the surface of the cell. Spectroelectrochemical IR measurements were performed on

dx.doi.org/10.1021/jo400026r | J. Org. Chem. 2013, 78, 2853−2862

10^{-3} M solutions of the compound and 0.4 M in $[NBu_4][BF_4]$ as supporting electrolyte and were prepared using Schlenk line techniques. Electrolysed solutions were transferred to sealed IR cells, via steel or Teflon canula, for analysis by IR spectroscopy.

DFT Calculations. DFT calculations were performed on models of **1a** and **2a** as neutral, singly reduced, and direduced molecules in order to complement observations made in the EPR and to simulate IR and UV/vis experiments. The geometry optimizations and frequency calculations of the models were performed without any restraints using the B3LYP functional and 6-31g**[30] basis set for all atoms. Calculations of the EPR hyperfine couplings were performed using the B3LYP functional and a 6-31g** basis set for all atoms or a EPR-III basis set for all atoms apart from sulfur for which the 6-31g** basis set was used. This approach was taken because of the unavailability of EPR-III basis for atoms heavier than fluorine.[31] TDDFT calculations were performed with the B3LYP and PBE0[32] functionals and a 6-31g**basis set for all atoms. A PCM solvation model was also employed in these TDDFT calculations.[33] The calculated IR stretching frequencies for **1a** and **2a** were scaled by 0.96. All calculations were performed with Gaussian 03 Revision D. 01.[34]

■ ASSOCIATED CONTENT

Ⓢ Supporting Information

Additional experimental details, original ^1H, ^{13}C NMR spectra and mass spectra for **1a** and **1b**, full UV−vis and EPR data for all the oxidation and reduction processes, and further details of DFT calculations. Details of structural refinement and X-ray structures (CIF), structure packing diagrams. This material is available free of charge via the Internet at http://pubs.acs.org.

■ AUTHOR INFORMATION

Corresponding Author

*E-mail: neil.champness@nottingham.ac.uk.

Notes

The authors declare no competing financial interest.

■ ACKNOWLEDGMENTS

We gratefully acknowledge the support of the Engineering and Physical Sciences Research Council (EP/H010432/1) and the University of Nottingham. N.R.C. gratefully acknowledges receipt of a Royal Society Wolfson Merit Award.

■ REFERENCES

(1) Würthner, F. *Chem. Commun.* **2004**, 1564.

(2) Schmidt, R.; Hak Oh, J.; Sun, Y.-S.; Deppisch, M.; Krause, A.-M.; Radacki, K.; Braunschweig, H.; Könemann, M.; Erk, P.; Bao, Z.; Würthner, F. *J. Am. Chem. Soc.* **2009**, *131*, 6215.

(3) Mikroyannidis, J. A.; Stylianakis, M. M.; Suresh, P.; Sharma, G. D. *Sol. Energy Mater. Sol. Cells* **2009**, *93*, 1792.

(4) Vân Anh, N.; Schlosser, F.; Groeneveld, M. M.; van Stokkum, I. H. M.; Würthner, F.; Williams, R. M. *J. Phys. Chem. C* **2009**, *113*, 18358.

(5) Baumstark, B.; Wagenknecht, H.-A. *Angew. Chem., Int. Ed.* **2008**, *47*, 2612.

(6) Wicklein, A.; Lang, A.; Muth, M.; Thelakkat, M. *J. Am. Chem. Soc.* **2009**, *131*, 14442.

(7) (a) Theobald, J. A.; Oxtoby, N. S.; Phillips, M. A.; Champness, N. R.; Beton, P. H. *Nature* **2003**, *424*, 1029. (b) Swarbrick, J. C.; Ma, J.; Theobald, J. A.; Oxtoby, N. S.; O'Shea, J. N.; Champness, N. R.; Beton, P. H. *J. Phys. Chem. B* **2005**, *109*, 12167. (c) Theobald, J. A.; Oxtoby, N. S.; Champness, N. R.; Beton, P. H.; Dennis, T. J. S. *Langmuir* **2005**, *21*, 2038. (d) Perdigão, L. M. A.; Perkins, E. W.; Ma, J.; Staniec, P. A.; Rogers, B. L.; Champness, N. R.; Beton, P. H. *J. Phys. Chem. B* **2006**, *110*, 12539. (e) de Feyter, S.; Miura, A.; Yao, S.; Chen, Z.; Würthner, F.; Jonkheijm, P.; Schenning, A. P. H. J.; Meijer, E. W.; de Schryver, F. C. *Nano Lett.* **2005**, *5*, 77. (f) Perdigao, L. M. A.; Saywell, A.; Fontes, G. N.; Staniec, P. A.; Goretzki, G.; Phillips, A. G.; Champness, N. R.; Beton, P. H. *Chem.—Eur. J.* **2008**, *14*, 7600. (g) Saywell, A.; Magnano, G.; Satterley, C. J.; Perdigão, L. M. A.; Britton, A. J.; Taleb, N.; Giménez-López, M. C.; Champness, N. R.; O'Shea, J. N.; Beton, P. H. *Nature Commun.* **2010**, *1*, 75.

(8) (a) Goretzki, G.; Davies, E. S.; Argent, P. S.; Warren, J. E.; Blake, A. J.; Champness, N. R. *Inorg. Chem.* **2009**, *48*, 10264. (b) Goretzki, G.; Davies, E. S.; Argent, S. P.; Alsindi, W. Z.; Blake, A. J.; Warren, J. E.; McMaster, J.; Champness, N. R. *J. Org. Chem.* **2008**, *73*, 8808. (c) Jimenez, A. J.; Spanig, F.; Rodrıguez-Morgade, M. S.; Ohkubo, K.; Fukuzumi, S.; Guldi, D. M.; Torres, T. *Org. Lett.* **2007**, *9*, 2481. (d) Dubey, R. K.; Efimov, A.; Lemmetyinen, H. *Chem. Mater.* **2011**, *23*, 778. (e) Chamberlain, T. W.; Davies, E. S.; Khlobystov, A. N.; Champness, N. R. *Chem.—Eur. J.* **2011**, *17*, 3759. (f) Slater, B. J.; Davies, E. S.; Argent, S. P.; Nowell, H.; Lewis, W.; Blake, A. J.; Champness, N. R. *Chem.—Eur. J.* **2011**, *17*, 14746.

(9) Langhals, H. *Heterocycles* **1995**, *40*, 477.

(10) Würthner, F.; Stepanenko, V.; Chen, Z.; Saha-Möller, C. R.; Kocher, N.; Stalke, D. *J. Org. Chem.* **2004**, *69*, 7933.

(11) (a) Pollard, A. J.; Perkins, E. W.; Smith, N. A.; Saywell, A.; Goretzki, G.; Phillips, A. G.; Argent, S. P.; Sachdev, H.; Müller, F.; Hüfner, S.; Gsell, S.; Fischer, M.; Screck, M.; Osterwalder, J.; Greber, T.; Berner, S.; Champness, N. R.; Beton, P. H. *Angew. Chem., Int. Ed.* **2010**, *49*, 1794. (b) Phillips, A. G.; Perdigão, L. M. A.; Beton, P. H.; Champness, N. R. *Chem. Commun.* **2010**, *46*, 2775.

(12) Langhals, H.; Demmig, S.; Huber, H. *Spectrochim. Acta* **1988**, *44A*, 1189.

(13) (a) Ramanan, C.; Smeigh, A. L.; Anthony, J. E.; Marks, T. J.; Wasielewski, M. R. *J. Am. Chem. Soc.* **2012**, *134*, 386. (b) Prusakova, V.; McCusker, C. E.; Castellano, F. N. *Inorg. Chem.* **2012**, *51*, 8589. (c) Vagnini, M. T.; Smeigh, A. L.; Blakemore, J. D.; Eaton, S. W.; Schley, N. D.; D'Souza, F.; Crabtree, R. H.; Brudvig, G. W.; Co, D. T.; Wasielewski, M. R. *Proc. Natl. Acad. Sci. U.S.A.* **2012**, *109*, 15651. (d) Jiménez, A. J.; Grimm, B.; Gunderson, V. L.; Vagnini, M. T.; Calderon, S. K.; Rodríguez-Morgade, M. S.; Wasielewski, M. R.; Guldi, D. M.; Torres, T. *Chem.—Eur. J.* **2011**, *17*, 5024. (e) Schlosser, F.; Sung, Y.; Kim, P.; Kim, D.; Würthner, F. *Chem. Sci.* **2012**, *3*, 2778. (f) Berberich, M.; Natali, M.; Spenst, P.; Chiorboli, C.; Scandola, F.; Würthner, F. *Chem.—Eur. J.* **2012**, *18*, 13651.

(14) (a) Iden, R.; Seybold, G. (BASF AG), German Patent Application DE 3434059 A1, 1985; *Chem. Abstr.* **1985**, *103*, 38696q. (b) Böhm, A.; Arms, H.; Henning, G.; Blaschka, P. (BASF AG), German Patent Application DE 19547209 A1, 1997; *Chem. Abstr.* **1997**, *127*, 96569g.

(15) (a) Nolde, F.; Pisula, W.; Mueller, S.; Kohl, C.; Müllen, K. *Chem. Mater.* **2006**, *18*, 3715. (b) Ahrens, M. J.; Tauber, M. J.; Wasielewski, M. R. *J. Org. Chem.* **2006**, *71*, 2107.

(16) (a) Zhao, C.; Zhang, Y.; Li, R.; Li, X.; Jiang, J. *J. Org. Chem.* **2007**, *72*, 2402. (b) Liang, B.; Zhang, Y.; Wang, Y.; Xu, W.; Li, X. *J. Mol. Struct.* **2009**, *917*, 113.

(17) Kosugi, M.; Shimizu, T.; Migita, T. *Chem. Lett.* **1978**, 13.

(18) Raisanen, M. T.; Slater (nee Phillips), A. G.; Champness, N. R.; Buck, M. *Chem. Sci.* **2012**, *3*, 84.

(19) Lin, M.-J.; Jiménez, Á.J.; Burschka, C.; Würthner, F. *Chem. Commun.* **2012**, *48*, 12050.

(20) Osswald, P.; Würthner, F. *J. Am. Chem. Soc.* **2007**, *129*, 14319.

(21) Safont-Sempere, M. M.; Osswald, P.; Stolte, M.; Grüne, M.; Renz, M.; Kaupp, M.; Radacki, K.; Braunschweig, H.; Würthner, F. *J. Am. Chem. Soc.* **2011**, *133*, 9580.

(22) Lee, S. K.; Zu, Y.; Herrmann, A.; Geerts, Y.; Müllen, K.; Bard, A. J. *J. Am. Chem. Soc.* **1999**, *121*, 3513.

(23) (a) Chis, V.; Mile, G.; Stiufiuc, R.; Leopold, N.; Oltean, M. *J. Mol. Struct.* **2009**, *47*, 924−926. (b) Menikh, A.; Bouraoui, A. *J. Mol. Struct.* **1997**, *403*, 189.

(24) Liang, B.; Zhang, Y.; Wang, Y.; Xu, W.; Li, X. *J. Mol. Struct.* **2009**, *917*, 133.

(25) Wong, M. W. *Chem. Phys. Lett.* **1996**, *256*, 391.

(26) Sazanovich, I. V.; Alamiry, M. A. H.; Best, J.; Bennett, R. D.; Bouganov, O. V.; Davies, E. S.; Grivin, V. P.; Meijer, A. J. H. M.;

Plyusnin, V. F.; Ronayne, K. L.; Shelton, A. H.; Tikhomirov, S. A.; Towrie, M.; Weinstein, J. A. *Inorg. Chem.* **2008**, *47*, 10432. Taylor, A. J.; Davies, E. S.; Weinstein, J. A.; Sazanovich, I. V.; Bouganov, O. V.; Tikhomirov, S. A.; Towrie, M.; McMaster, J.; Garner, C. D. *Inorg. Chem.* **2012**, *51*, 13181.
(27) Kubas, J. *Inorg. Synth.* **1990**, *28*, 68.
(28) Gagné, R. R.; Koval, C. A.; Lisensky, G. C. *Inorg. Chem.* **1980**, *19*, 2854.
(29) Macgregor, S. A.; McInnes, E.; Sorbie, R. J.; Yellowlees, L. J. In *Molecular Electrochemistry of Inorganic, Bioinorganic and Organometallic Compounds*; Pombeiro, A. J. L., McCleverty, J. A., Eds.; Kluwer Academic Publishers: Dordrecht, 1993; p 503.
(30) Ditchfield, R.; Hehre, W. J.; Pople, J. A. *J. Chem. Phys.* **1971**, *54*, 724.
(31) Barone, V. *Recent Advances in Density Functional Methods, Part I*, 1996, Chong, D. P., Ed.; World Scientific Publ. Co.: Singapore, 1996.
(32) Adamo, C.; Barone, V. *J. Chem. Phys.* **1999**, *110*, 6158.
(33) Tomasi, J.; Mennucci, B.; Cammi, R. *Chem. Rev.* **2005**, *105*, 2999.
(34) Frisch, M. J.; Trucks, G. W.; Schlegel, H. B.; Scuseria, G. E.; Robb, M. A.; Cheeseman, J. R.; Zakrzewski, V. G.; Montgomery, J. A., Jr.; Stratmann, R. E.; Burant, J. C.; Dapprich, S.; Millam, J. M.; Daniels, A. D.; Kudin, K. N.; Strain, M. C.; Farkas, O.; Tomasi, J.; Barone, V.; Cossi, M.; Cammi, R.; Mennucci, B.; Pomelli, C.; Adamo, C.; Clifford, S.; Ochterski, J.; Petersson, G. A.; Ayala, P. Y.; Cui, Q.; Morokuma, K.; Malick, D. K.; Rabuck, A. D.; Raghavachari, K.; Foresman, J. B.; Cioslowski, J.; Ortiz, J. V.; Stefanov, B. B.; Liu, G.; Liashenko, A.; Piskorz, P.; Komaromi, I.; Gomperts, G.; Martin, R. L.; Fox, D. J.; Keith, T.; Al-Laham, M. A.; Peng, C. Y.; Nanayakkara, A.; Gonzalez, C.; Challacombe, M.; Gill, P. M. W.; Johnson, B. G.; Chen, W.; Wong, M. W.; Andres, J. L.; Head-Gordon, M.; Replogle, E. S.; Pople, J. A. *Gaussian 03 Revision D. 01*; Gaussian, Inc., Wallingford, CT, 2004.